

# Thermalization of photoexcited localized excitons in GaSe samples with stacking disorder

Vito Capozzi

*Dipartimento di Fisica, Università degli Studi di Bari, via Amendola 173, I-70126 Bari, Italy  
and Centro Studi del Consiglio Nazionale delle Ricerche, Unità C.I.S.M. I-38050 Povo (Trento), Italy*

Klaus Maschke

*Institut de Physique Appliquée, Ecole Polytechnique Fédérale de Lausanne, CH-1015 Lausanne, Switzerland  
(Received 31 January 1986)*

We have studied the photoluminescence of GaSe at 80 K under energy-selective excitation conditions. For excitation energies on the low-energy side of the  $n = 1$  direct free-exciton absorption line we find that the emission line due to the  $n = 1$  direct free excitons follows rigidly the excitation energy, whereas for excitation energies on the high-energy side the respective emission spectrum shifts to lower energies and the linewidth increases. Similar behavior is found on exciting into the excited  $n = 2$  direct exciton states. At room temperature and for excitation energies larger than the direct gap the emission spectra become independent of the excitation energy. We show that the experimental findings can be understood in terms of an extended version of the multiple-trapping model, which accounts for the localization of excitons in the direction perpendicular to the layers of GaSe. This localization is a consequence of the stacking disorder present in our samples. The resulting physical picture is that at low temperatures and for low excitation energies thermalization effects can be neglected within the recombination lifetime, whereas at high temperatures or high excitation energies the thermalization takes place within the recombination lifetime.

## I. INTRODUCTION

The study of energy-transfer and relaxation processes in nonequilibrium systems is of fundamental interest, as well from the theoretical as from the experimental point of view. Photoluminescence (PL) experiments provide a convenient tool to study the energy distribution of excited particles, and are therefore very important for the study of the above problem, in particular, if localized states are involved. Recently, several groups have reported on PL experiments with energy-selective excitation.<sup>1-3</sup> Such experiments are particularly useful when one excites into the exciton bands, since in this case the initial states in which the excitons are generated before thermalization have all the same energy. It is thus possible to study the nature of the initial states through the dependence of the PL on the initial-state energy. Different systems have been investigated in this way: (i) alloy systems like  $\text{CdS}_x\text{Se}_{1-x}$ ,<sup>1</sup> (ii) quantum well systems like  $\text{GaAs-Al}_x\text{Ga}_{1-x}\text{As}$ ,<sup>2</sup> and (iii) layer-compound systems like GaSe.<sup>3</sup> In all three cases we have some kind of disorder, which leads to at least partial localization of the exciton states: chemical disorder in case (i), fluctuation of the well thickness in case (ii), and stacking disorder in case (iii). It is thus not surprising that the experimental findings are rather similar for the three systems: For excitations in the energy range of the direct exciton absorption the linewidth of the exciton-emission line increases considerably with the excitation energy. Different models have been proposed to understand this behavior of the PL spectra.<sup>1,4</sup> They result in a picture where exciton states near the minimum of the exciton band are localized due to Anderson localization, whereas excitons at higher energy remain mobile.

In the present contribution we concentrate on the case of GaSe, which is theoretically appealing because the stacking disorder can be described as a one-dimensional (1D) disorder problem, as was shown in Refs. 5 and 6. We first present the experimental evidence for the dependence of the PL on the excitation energy. Besides the increase of the linewidth of the exciton-emission line, we find that the peak of the exciton-emission spectrum follows rigidly the excitation energy when exciting into the low-energy tail of the  $n = 1$  direct free exciton-absorption line. We then present a simple model for the description of the PL in the case of stacking disorder. This model is inspired from the extended multiple-trapping model which was developed for the description of the time decay of the PL in the case of  $\alpha$ -Si.<sup>7</sup> The successful description of our experimental results indicates that the localization of the free excitons due to stacking disorder is in fact responsible for the observed effects. We mention that additional experimental support for the localization of excitons in GaSe can be found in Ref. 8.

## II. EXPERIMENTAL TECHNIQUES

The GaSe crystals were grown from the melt by the Bridgman technique.<sup>9</sup> The samples were not intentionally doped. Their electrical conductivity is of  $p$  type with  $N_A - N_D \simeq 10^{15} \text{ cm}^{-3}$  and  $N_A + N_D \simeq 10^{17} \text{ cm}^{-3}$ , where  $N_A$  and  $N_D$  are the acceptor and donor concentrations.<sup>10</sup> X-ray studies and transmission spectra show that our crystals contain stacking faults, and that the predominant stacking is of the  $\epsilon$  type.<sup>11</sup> The ingots were cleaved along the planes of the layers. The obtained slices, which were about 0.1 mm thick, were attached to a copper cold finger

of a cryostat. The temperature of the cryostat could vary from 2 to 300 K.

The surface of the samples was illuminated in a direction forming a  $45^\circ$  angle with respect to the  $c$  axis by a cw dye laser with a bandwidth smaller than  $0.5 \text{ cm}^{-1}$  and fed with rhodamine 6G. It was pumped by an Ar-ion laser. The dye laser was used as a monochromatic light source for the selective PL spectra. The excitation intensity was of the order of  $1 \text{ W cm}^{-2}$ . The light beam was focused on a spot with a diameter of about  $100 \mu\text{m}$ . Two crossed polaroids placed before and after the sample were used in order to prevent the reflection of the background luminescence of the dye. The emission light was collected from the excited front face of the sample and analyzed by a double spectrometer having a very weak straylight, such that we could measure the PL response at energies very close to the excitation laser line, i.e., closer than  $10 \text{ cm}^{-1}$ . Special care was taken to prevent detection of the resonant scattering of the excitation light: during the scanning of the spectrometer, the recording of the emission light was stopped in a range of about  $1 \text{ meV}$  across the laser excitation energy. The signal detected by a cooled photomultiplier was recorded using photon-counting techniques. The data were sent to a computer for storage and data processing.

### III. EXPERIMENTAL RESULTS

Some typical PL spectra of GaSe measured at 80 K are shown in Fig. 1. The presented spectra were obtained for different excitation energies within the absorption line of the direct  $n = 1$  exciton. The absorption coefficient of the same sample is given in Fig. 2 for  $E \perp c$ . Each of the spectra consists of four structures which can be related to contributions from the direct free excitons (DFE's), the direct bound excitons (DBE's), the indirect free excitons (IFE's), and the indirect bound excitons (IBE's).<sup>12,13</sup> For excitations in the low-energy tail of the DFE absorption line, which is centered at  $2.098 \text{ eV}$  ( $17920 \text{ cm}^{-1}$ ), we find that the DFE luminescence line follows rigidly the excitation energy (curves *a*, *b*, and *c*). This behavior can be observed in a range of  $12 \text{ meV}$ . It indicates, that a large portion of the excitons which are generated in the low-energy tail states remains in these states within the period of the radiative lifetime. For excitation energies on the high-energy side of the DFE absorption line the DFE luminescence is shifted to lower energies. In this case the linewidth of the DFE line, which is measured by its half-width, is increased considerably: It is about twice the width found for low excitation energies. Finally, the PL spectra become completely independent of the excitation energy for excitation energies larger than the direct gap.

In Fig. 1, the small structure on the high-energy side of the DFE emission, which is enhanced when exciting into the high-energy tail of the  $n = 1$  exciton line, is attributed to the contribution of the  $n = 2$  exciton states, since the separation in energy between the  $n = 1$  and the  $n = 2$  excitons is  $15 \text{ meV}$ . It is interesting to note that for optical excitation within the  $n = 2$  exciton line the  $n = 2$  PL shows the same behavior as discussed above for the case of  $n = 1$ . This indicates that the  $n = 2$  excitons relax similarly to the  $n = 1$  excitons and that the relaxation to-

wards lower-energy states is still rather slow.

The discussed dependence of the DFE-PL spectra on the excitation energy is resumed in Figs. 3(a) and 3(b). Figure 3(a) shows the dependence of the position of the DFE line on the excitation energy, whereas the energy dependence of the linewidth is shown in Fig. 3(b). We see that the linewidth is equal to  $6 \text{ meV}$  for low excitation en-

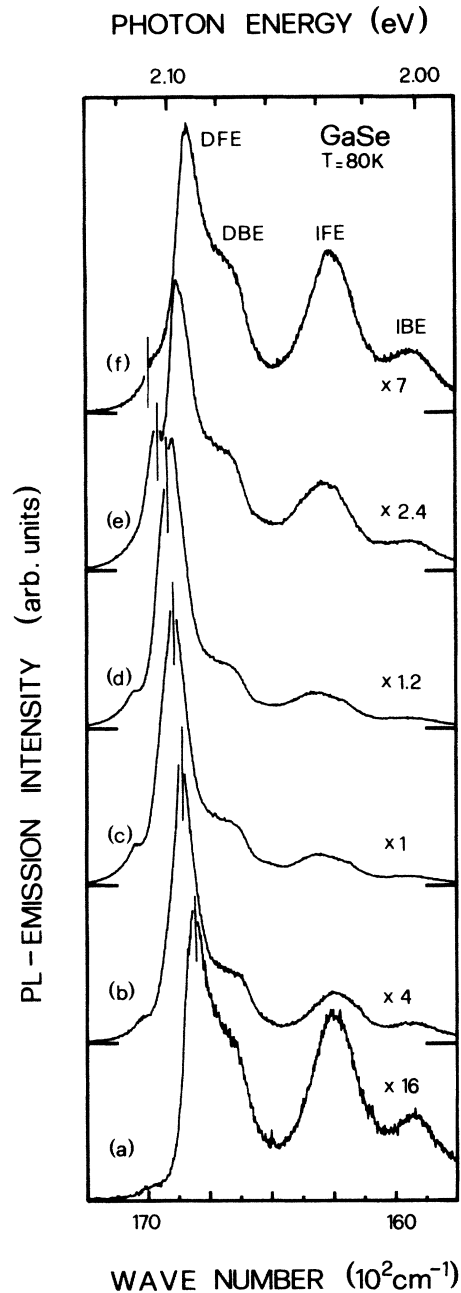


FIG. 1. Energy-selective photoluminescence spectra of GaSe measured at 80 K for an excitation energy of  $5 \text{ W cm}^{-2}$ . Curves *a* to *f* were obtained for different laser frequencies: curve (a)  $16850 \text{ cm}^{-1}$ ; curve (b)  $16890 \text{ cm}^{-1}$ ; curve (c)  $16920 \text{ cm}^{-1}$ ; curve (d)  $16936 \text{ cm}^{-1}$ ; curve (e)  $16966 \text{ cm}^{-1}$ ; and curve (f)  $17000 \text{ cm}^{-1}$ . The vertical lines indicate the excitation energies corresponding to the different curves. The spectral resolution is  $5 \text{ cm}^{-1}$ . The amplification factor is indicated for each spectrum. For the denomination of the lines, see text.

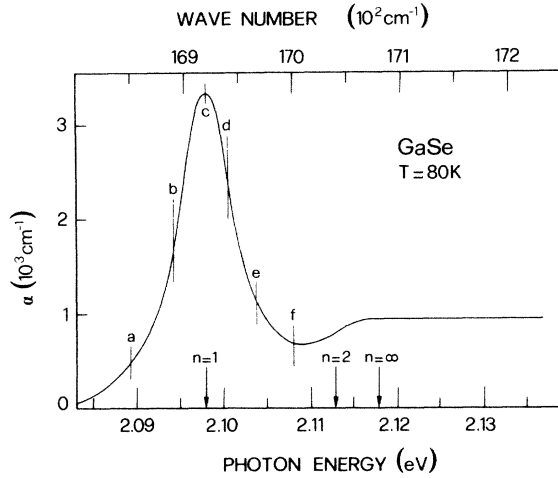


FIG. 2. Absorption spectrum for the sample of the Fig. 1, measured at 80 K and for light propagating parallel to the  $c$  axis of the crystal. The vertical lines indicate the excitation energies at which the six spectra of Fig. 1 were measured. The position of the direct exciton states  $n=1$ ,  $n=2$ , and  $n=\infty$  is indicated by arrows. The spectral resolution is  $6 \text{ cm}^{-1}$ .

ergies and increases with increasing energy. It saturates at about 12 meV for excitation energies above the band gap.

We mention that the PL linewidth is sample dependent: In high-quality GaSe samples the emission lines are rather narrow (6 meV instead of 12 meV). The dependence of the DFE line on the excitation energy is also much less pronounced in these samples.

The PL spectrum measured at room temperature is shown in Fig. 4 for an excitation energy of 2.046 eV. At this temperature the bound excitons are completely dissociated. Therefore only the DFE and IFE lines persist in the PL spectrum. The energy shift of the PL spectrum to lower energies is due to the shrinkage of the gap with increasing temperature.<sup>14</sup> At this temperature no shift of the DFE line is observed when we tune the laser energy inside its energy range. Moreover, the linewidth of the DFE emission remains constant. Its absolute value, however, which is about 33 meV, is much larger than that observed at 80 K.

#### IV. EXCITONS IN THE PRESENCE OF STACKING DISORDER

In layer materials like GaSe the individual layers are usually stacked in a rather stochastic manner, such that the crystal loses its translational symmetry along the crystallographic  $c$  axis, whereas it remains invariant for primitive translations parallel to the layers. This stacking disorder strongly influences the properties of the electronic states near the band edges<sup>5</sup> as well as the exciton states.<sup>6</sup> In the following we will only consider the exciton band corresponding to the  $n=1$  direct excitons. Furthermore, we shall only be interested in the behavior of the exciton states near the bottom of the exciton band, which lies at  $\mathbf{K}=0$  in the ordered case.

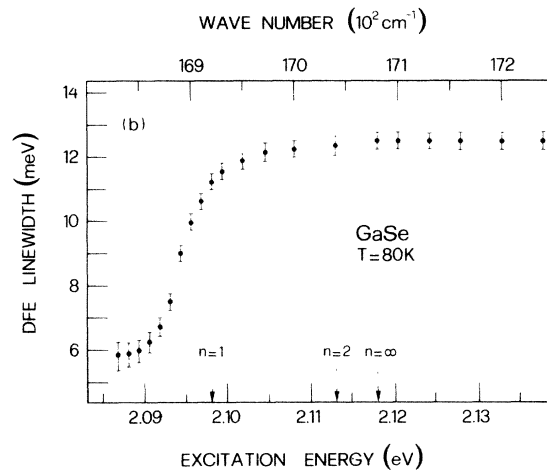
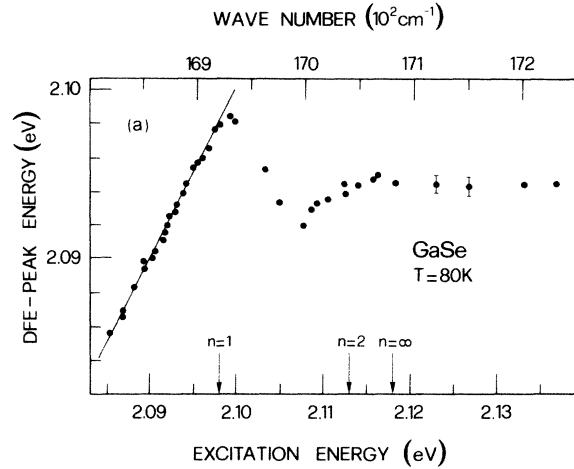


FIG. 3. (a) Energy position of the emission line of the direct free exciton  $n=1$  (DFE) versus the excitation energy. The straight line indicates the energy region in which the DFE emission peak is resonant with the excitation energy. (b) Linewidth of the DFE emission line versus the excitation energy. In both figures the positions of the direct exciton states  $n=1$ ,  $n=2$ , and  $n=\infty$  are indicated by arrows. All the data were obtained at  $T=80 \text{ K}$  and for a laser intensity of  $5 \text{ W cm}^{-2}$ .

The influence of the stacking disorder on the  $n=1$  exciton states can be described within the effective-mass approximation, as was shown in Ref. 6. The energies of the exciton states which are given by the dispersion relation  $E(\mathbf{K})$  or  $E(\mathbf{K}_{\parallel}, \mathbf{K}_{\perp})$  in the ideal-crystal case, then become

$$E(i, \mathbf{K}_{\perp}) = \delta_i + \varepsilon(\mathbf{K}_{\perp}), \quad (1)$$

where  $\mathbf{K}_{\perp}$  is the  $\mathbf{K}$  vector which describes the motion of the center of mass of the excitons along the layers and the index  $i$  replaces the  $\mathbf{K}_{\parallel}|c$  component of the  $\mathbf{K}$  vector in the ordered case.  $\varepsilon(\mathbf{K}_{\perp})$  describes thus a two-dimensional (2D)-band which has a quadratic dispersion near the band minimum at  $\mathbf{K}_{\perp}=0$ . The energies  $\delta_i$  are distributed according to a 1D density of states, which is obtained from a 1D disordered chain Hamiltonian. In principle, the

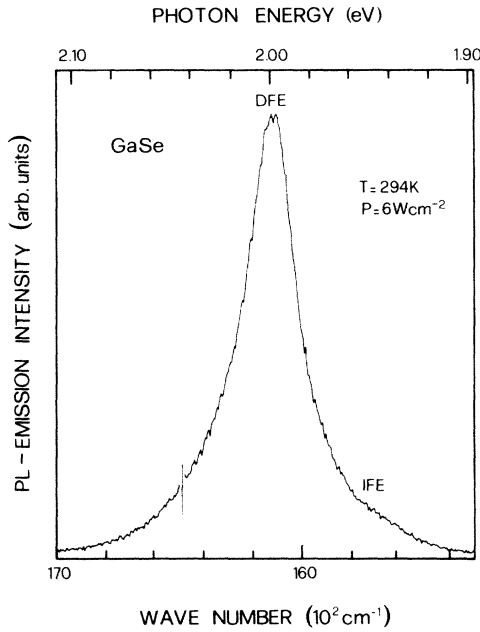


FIG. 4. Photoluminescence spectrum of GaSe measured at room temperature. The sample is the same as the one used for the previous figures. At this temperature the photoluminescence spectra are practically independent of the excitation energy, is explained in the text. The presented curve is obtained for the excitation energy 2.046 eV ( $16497 \text{ cm}^{-1}$ ), as indicated by the vertical line. The laser intensity is  $6 \text{ W cm}^{-2}$ , and the spectral resolution is  $10 \text{ cm}^{-1}$ .

latter will depend on  $\mathbf{K}_\perp$ , and so will  $\delta_i$ . However, since we are only interested in the properties of the exciton states near the band edges, we may neglect this  $\mathbf{K}_\perp$  dependence.

As shown in Ref. 6, the eigenfunctions which describe the exciton states may be written

$$\Psi_{i\mathbf{K}_\perp}(\mathbf{r}, \mathbf{R}) = \varphi(\mathbf{r}, \mathbf{R}) L_{i\mathbf{K}_\perp}(\mathbf{R}), \quad (2)$$

where  $\mathbf{r}$  describes the relative distance between electron and hole, and  $\mathbf{R}$  describes the position of the center of mass. The function  $\varphi$  describes the relative motion of electron and hole and depends only weakly on  $\mathbf{R}$ , whereas  $L_{i\mathbf{K}_\perp}(\mathbf{R})$  describes the behavior of the center of mass. In the case of the perfect crystal  $L_{i\mathbf{K}_\perp}(\mathbf{R})$  would just be described by a plane wave, i.e.,

$$L_{i\mathbf{K}_\perp, cr}(\mathbf{R}) = (1/\sqrt{\Omega}) \exp(i\mathbf{K} \cdot \mathbf{R}). \quad (3)$$

In the case of stacking disorder we will have mixing of the above plane waves corresponding to different  $\mathbf{K}_\parallel$  and therefore obtain

$$\begin{aligned} L_{i\mathbf{K}_\perp}(\mathbf{R}) &= \frac{1}{\sqrt{\Omega}} \sum_{\mathbf{K}_\parallel} c_i(\mathbf{K}_\parallel) e^{i\mathbf{K}_\perp \cdot \mathbf{R}_\perp} e^{i\mathbf{K}_\parallel \cdot \mathbf{z}} \\ &= \frac{1}{\sqrt{\Omega}} e^{i\mathbf{K}_\perp \cdot \mathbf{R}_\perp} L_i(z). \end{aligned} \quad (4)$$

$\mathbf{R}_\perp$  is the projection of the vector  $\mathbf{R}$  on the layer plane. As in the expression for the energy we have again neglected any dependence of the coefficients  $c_i$  on the wave vector  $\mathbf{K}_\perp$ . From the  $\mathbf{K}$  selection rules for optical transitions in the ideal crystal it follows immediately that in the disordered case the optical transition probability is proportional to  $|c_i(\mathbf{K}_\parallel=0)|^2$ , i.e., in the presence of stacking disorder even states which are somewhat above the bottom of the exciton band can be reached by optical transitions. Another consequence of the stacking disorder is the localization of exciton states in the direction of the  $c$  axis. This follows immediately from the fact that the functions  $L_{i\mathbf{K}_\perp}(\mathbf{R})$  are eigenfunctions of a Hamiltonian, which describes a disordered 1D chain.<sup>6</sup> Excitons can thus move freely through the crystal along the layers, whereas their center of mass is localized in the direction perpendicular to the layers. It is this property which is responsible for the experimental features discussed in Sec. III, as will be shown in Sec. V.

## V. TRANSITION RATES

We have seen in Sec. IV that near the bottom of the exciton band the motion of the center of mass is described by the function  $L_{i\mathbf{K}_\perp}(\mathbf{R})$ , Eq. (4). The corresponding eigenvalues of the exciton states are given by Eq. (1). The index  $i$  stays for (i) the contribution  $\delta_i$  to the energy  $E(i, \mathbf{K}_\perp)$ , (ii) the position of the state along the  $c$  direction, which can be represented by the center of localization  $z_s$ . In order to specify these two features we shall in the following replace the index  $i$  by "is" where  $i$  defines  $\delta_i$ , and  $s$  denotes the localization center of the state. We shall further assume that the excitons are in thermal equilibrium in each 2D band  $is$ . This supposes that the transitions between exciton states within an exciton band are much faster than transitions between states belonging to different bands. This is a reasonable assumption since the transitions between states of different bands are generally less probable because of the small spatial overlap between the involved wave functions. Describing the equilibrium distribution of excitons by the Boltzmann statistics we thus define for each band

$$n_{is, \mathbf{K}_\perp} = \frac{\tilde{n}_{is}}{g_2 k_B T} \exp \left[ - \frac{\hbar^2 \mathbf{K}_\perp^2}{2m k_B T} \right], \quad (5)$$

where  $n_{is, \mathbf{K}_\perp}$  is the number of excitons in the state  $|is, \mathbf{K}_\perp\rangle$ ,  $\tilde{n}_{is}$  is the total number of excitons in this band,  $g_2$  is the 2D density of states, which is constant near the band edge, and  $m$  is the exciton mass in the layer plane. The transition rate between states  $|is, \mathbf{K}_\perp\rangle$  and  $|jt, \mathbf{K}'_\perp\rangle$  of different bands  $is$  and  $jt$  can be described by

$$t_{is, jt}(\mathbf{K}_\perp, \mathbf{K}'_\perp) = C n_{is, \mathbf{K}_\perp} O_{is\mathbf{K}_\perp, jt\mathbf{K}'_\perp} f[E(i, \mathbf{K}_\perp), E(j, \mathbf{K}'_\perp), T], \quad (6)$$

where

$$f(E(i, \mathbf{K}_1), E(j, \mathbf{K}'_1), T) = \begin{cases} e^{-[E(j, \mathbf{K}'_1) - E(i, \mathbf{K}_1)]/k_B T} & \text{if } E(j, \mathbf{K}'_1) > E(i, \mathbf{K}_1), \\ 1 & \text{otherwise.} \end{cases} \quad (7)$$

$O_{is\mathbf{K}_1, jt\mathbf{K}'_1}$  is the square of the spatial overlap between the two functions  $|is, \mathbf{K}_1\rangle$  and  $|jt, \mathbf{K}'_1\rangle$ , which is given by

$$O_{is\mathbf{K}_1, jt\mathbf{K}'_1} = \left[ \int dz |L_i(z - z_s)| |L_j(z - z_t)| \right]^2 = O_{is, jt}. \quad (8)$$

The functions  $L_i(z)$  are the localized functions described in Eq. (4). We note that within the above approximation the overlap matrix element is independent of  $\mathbf{K}_1$  and  $\mathbf{K}'_1$ . Starting from Eq. (6) we can therefore define a total transition rate  $t_{is, jt}$  from a 2D band  $is$  centered at  $z_s$  and with the bottom  $\delta_i$ , to a different 2D band  $jt$  which starts at  $\delta_j$  and is located at  $z_t$ . We thus obtain

$$t_{is, jt} = \int \int t_{is, jt}(\mathbf{K}_1, \mathbf{K}'_1) d^2\mathbf{K}_1 d^2\mathbf{K}'_1. \quad (9)$$

Here the integrals extend over the 2D hexagonal Brillouin zone. Since in the present work we deal with the luminescence properties rather than with transport properties, we need only know the energy distribution of the excitons, and thus may integrate over their spatial distribution. We thus define

$$t_{is, j} = \sum_t t_{is, jt} \quad (10)$$

which is the total transition rate for an exciton in band  $is$  at position  $z_s$  towards the ensemble of all bands  $jt$  with arbitrary spatial position. In the limit of perfect homogeneity this transition rate becomes independent of the initial position  $z_s$  of the excitons. We then obtain a spatially independent transition rate  $t_{ij}$  which depends only on the bottom energies  $\delta_i, \delta_j$  of the involved bands  $i$  and  $j$ ,

$$t_{ij} = t_{is, j}. \quad (11)$$

This latter approximation is obviously only valid if there are always a sufficient number of bands  $jt$  which overlap with  $is$ , such that the probability to find a spatially isolated band  $is$  becomes negligible. In the case of strong localization of the states and of a small density of states the above approximation will not hold. It is, however, easy to see that the assumption of homogeneity is only critical at very low temperatures, where transitions to higher energy states are impossible. We note that the eventual resulting error will be systematic and will always overestimate the transition rates.

Following the procedure described in Eqs. (5) to (11) we obtain after some straightforward but somewhat lengthy calculation

$$t_{ij} = CO_{ij}(|\delta_i - \delta_j| + 2k_B T) f_{ij}(T) g_1(E_j) \Delta E_j, \quad (12)$$

with

$$f_{ij}(T) = \begin{cases} e^{-(\delta_j - \delta_i)/k_B T} & \text{for } \delta_i < \delta_j, \\ 1 & \text{otherwise,} \end{cases} \quad (13)$$

where  $g_1(E)$  represents the 1D density of states which describes the distribution of the  $\delta_j$ 's, i.e.,  $g_1(E_j) \Delta E_j$  is the number of bands which correspond to the energies  $\delta_j$  such that

$$E_j - \frac{\Delta}{2} < \delta_j < E_j + \frac{\Delta}{2}. \quad (14)$$

The width  $\Delta$  of the energy intervals must be chosen sufficiently small, i.e.,  $\Delta \ll kT$ . Approximating the behavior of the functions  $L_i$  by

$$|L_i(z)| = (\beta_i)^{1/2} e^{-\beta_i |z|}, \quad (15)$$

where  $(\beta_i)^{1/2}$  guarantees the proper normalization, we obtain

$$O_{ij} = \frac{\beta_i \beta_j^5 - \beta_i^5 \beta_j - 5\beta_i^2 \beta_j^4 + 5\beta_i^4 \beta_j^2 - \beta_i^6 + \beta_j^6}{(\beta_i - \beta_j)^2 (\beta_i + \beta_j)^3 (\beta_j^2 - \beta_i^2)}. \quad (16)$$

For constant  $\beta$  this reduces to

$$O_{ij} = \frac{5}{8\beta}. \quad (17)$$

In Eqs. (16) and (17) we have neglected a constant prefactor which is taken into account in the constant  $C$  of Eq. (12).

## VI. STATIONARY EQUATIONS

Having defined the effective transition rate  $t_{ij}$  we can now write down the rate equations which describe the energy distribution of the excitons over the groups of bands labeled by the index  $i$  such that  $E_i - \Delta/2 < \delta_i < E_i + \Delta/2$ . For reasons of simplicity we will change the notation in the following, and call such a group of bands "states in interval  $i$ ." We obtain

$$\frac{dn_i}{dt} = -n_i \sum_j t_{ij} + \sum_j t_{ji} n_j - \frac{n_{i0}}{\tau_i} + \gamma_i. \quad (18)$$

$n_i$  ( $n_j$ ) is the number of excitons within the interval  $i$  ( $j$ ),  $n_{i0}$  is the number of optically accessible excitons at the bottom of the 2D band  $i$ ,  $\tau_i$  is the recombination lifetime of excitons in interval  $i$ , and  $\gamma_i$  is the generation rate of excitations in interval  $i$  by optical excitation. It is important to note that in spite of the 2D energy dispersion present in each "state," photons of a given energy can only reach one of the intervals  $i$ . This follows immediately from the conservation of the  $\mathbf{K}_1$  vector in the optical excitation process. For our present purpose we have to solve the above equations in the stationary limit, i.e., we have to solve the inhomogeneous linear equation system

$$-n_i \sum_j t_{ij} + \sum_j t_{ji} n_j - \frac{n_{i0}}{\tau_i} = -\gamma_i, \quad (19)$$

where  $\gamma_i = \gamma \delta_{ik}$ . For the numerical solution of the above

equations we have replaced the energies  $\delta_i$  within interval  $i$  by their mean value, i.e.,

$$\delta_i = (i + \frac{1}{2})\Delta . \quad (20)$$

We note that in Eqs. (18) and (19) we have neglected nonradiative transitions as well as transitions towards indirect and bound states. Therefore, our description does not cover the complete PL spectrum. We have found, however, that the inclusion of nonradiative transitions does not change the general behavior of the DFE emission, which is the principal concern of the present contribution.

## VII. THEORETICAL RESULTS

For our numerical calculations we set the width of the intervals equal to 1 meV. The 1D density of states  $g_1(E)$  is approximated by

$$g_1(E) \sim \frac{d + (E - E_0)^x}{A + (E - E_0)^{x+1/2}} \quad \text{for } E - E_0 > 0 , \quad (21)$$

with  $x=4$ ,  $d=704 \text{ meV}^x$ ,  $A=7820 \text{ meV}^{x+1/2}$ , and  $E_0=2.087 \text{ eV}$ . This form of  $g_1(E)$  allows us to describe the general behavior of the density of states of a weakly disordered 1D chain: The  $(E - E_0)^{-1/2}$  behavior is retained at large energies, and the Van Hove singularity at  $E_0$  is broadened by the disorder. In order to obtain the energy dependence of the reciprocal lifetime we start from the absorption coefficient which describes the optical transitions of the  $n=1$  direct exciton states,

$$\alpha(E) = \frac{W(E)E}{I(E)} . \quad (22)$$

$W(E)$  is the number of optical transitions per unit volume and unit time,  $E$  is the photon energy, and  $I(E)$  is the light intensity. For the considered energy range of excitonic luminescence  $E/I(E)$  remains practically constant. Therefore we can write

$$\frac{1}{\tau(E)} = \frac{W(E)}{g_1(E)\Delta} \sim \frac{\alpha(E)}{g_1(E)} \quad \text{for } E - E_0 > 0 . \quad (23)$$

$\alpha(E)$  is approximated by a Lorentzian of half-width 8 meV, which is in agreement with the width of the experimental absorption spectra in the presence of stacking disorder (see Fig. 2). The maximum of the absorption coefficient is placed at 11 meV above  $E_0$ , which is defined in Eq. (21). The dependence on energy of the reciprocal localization length  $\beta$  is described by

$$\beta(E) \sim \frac{1}{1 + q(E - E_0)} \quad \text{for } E - E_0 > 0 , \quad (24)$$

with  $q=10 \text{ meV}^{-1}$ . The constants of proportionality in Eqs. (21), (23), and (24) are included in the prefactor  $C$ , Eq. (12), which is set equal to  $4 \times 10^{-5} \text{ s}^{-1}$ . The individual  $\delta$ -function-like contributions to the PL are broadened by a Lorentzian of half-width  $\Gamma=3 \text{ meV}$ , which corrects for the temperature dependence of the intrinsic linewidth as well as for the discontinuous steps of our model density

of states, which result from the approximation in Eq. (20).

The functions  $g_1(E)$ ,  $\alpha(E)$ , and  $1/\tau(E)$  are shown in Fig. 5. In the ordered case  $1/\tau(E)$  would be a  $\delta$  function at  $E=E_0$ . Therefore, the behavior of  $1/\tau(E)$  shown in Fig. 5 can be understood as a broadening and a displacement of the  $\delta$  function due to disorder.

We note that the above choice of our parameters is completely empirical, and that the stacking disorder enters only in an indirect manner via its influence on the exciton states. It is thus difficult to draw quantitative conclusions on the stacking disorder itself. Nevertheless, it is interesting to recall the essential spatial parameters for the case of GaSe: The smallest possible length scale for the description of the stacking disorder is given by the layer thickness of 8 Å. This should be compared with the Bohr radius of the ground-state exciton, which is equal to 32 Å. The disorder potential which is effectively seen by the excitons, is obtained after an average over the exciton diameter.<sup>6</sup> The rather strong influence of the stacking disorder on the exciton states, which is given by Eqs. (21), (23), and (24), thus indicates that the disorder must already be present over the length scale of 5 to 10 layers.

The theoretical PL spectra are shown in Fig. 6 for  $T=80 \text{ K}$  and different excitation energies. The luminescence can be decomposed into two contributions: (i) the small-width primary contributions from the intervals in

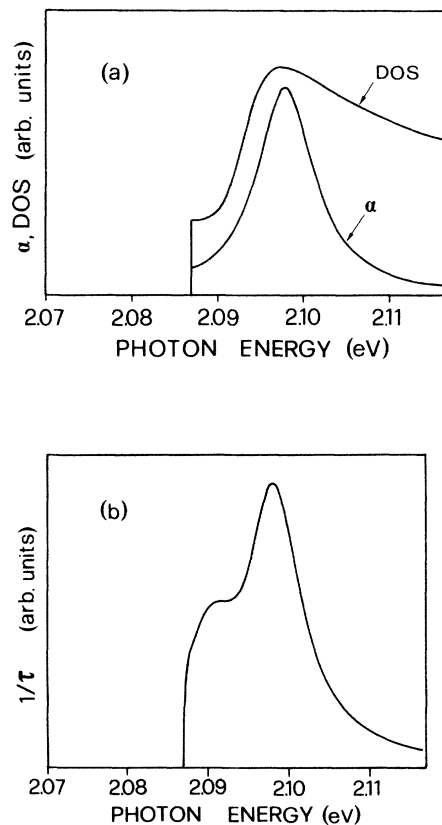


FIG. 5. Model functions of our calculations (a) 1D density of states (DOS), DFE absorption coefficient  $\alpha$  and (b) reciprocal lifetime  $1/\tau(E)$ .

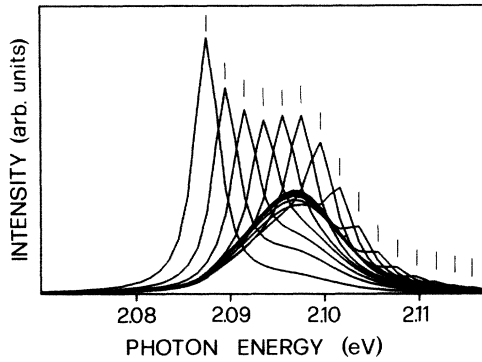


FIG. 6. Calculated photoluminescence spectra at 80 K for different excitation energies. The corresponding excitation energies are indicated by the vertical lines.

which the excitons are generated through optical excitation. This contribution was in part eliminated in the experimental spectra; (ii) the large-width secondary contributions which are due to excitons which have travelled through different states before recombination.

The theoretical curves are found to be in good agreement with experiment: At small excitation energies the PL spectra are dominated by the primary contributions. At larger excitation energies the secondary contributions become more and more important and build up a structure which is practically independent of the excitation energy and which has its maximum at about 10 meV above the bottom of the exciton band. The width of the secondary peak at large excitation energies is appreciably larger than the width of the luminescence spectrum at small excitation energies.

The position of the photoluminescence peak at the low-energy side as well as the half-width of this peak are shown in Figs. 7(a) and 7(b) as a function of the excitation energy. Comparison with the experimental results in Figs. 3(a) and 3(b) shows again a good overall agreement. The behavior of the calculated PL spectra remains qualitatively the same when the parameters are changed. In particular the "freezing in" of the initially excited excitons observed at low excitation energies is always present, as long as the constant  $C$  in Eq. (12) is kept sufficiently small. However, the position of the critical energy, at which the secondary excitation luminescence becomes important, changes, and becomes in general larger.

Experimentally we observe also a change in the position of the DFE line when we excite into the  $n=2$  exciton states [see Fig. 3(a)]. The situation is similar to that found for excitation into the  $n=1$  band: For excitations into the low-energy side of the  $n=2$  band the energy of the DFE line increases with the excitation energy, whereas for excitations into the high-energy side of the  $n=2$  band the DFE line becomes independent of the laser energy. It is obvious that this feature cannot be reproduced directly by our model, since it does not contain any  $n=2$  states. The similar behavior suggests, however, that the energies and the spatial positions of the  $n=1$  states and the  $n=2$  states are strongly correlated: The experimental behavior

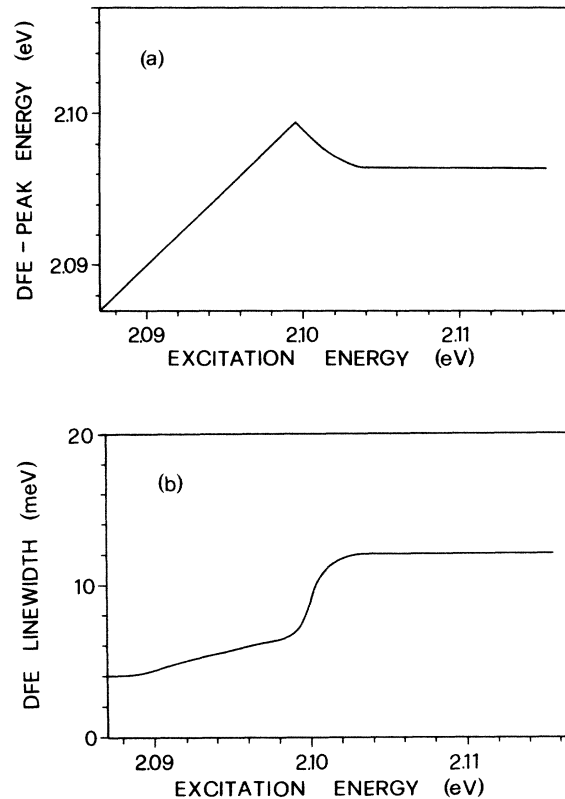


FIG. 7. (a) Position of the calculated DFE photoluminescence peak at the low-energy side of the photoluminescence spectrum as a function of the excitation energy. (b) Half-width of the calculated DFE photoluminescence peak as a function of the excitation energy.

can easily be explained if we assume that the distance in energy between overlapping  $n=1$  and  $n=2$  states is always equal to  $\frac{3}{4}$  Ry, i.e., 15 meV. In this case, excitons which are generated in the low-energy side of the  $n=2$  exciton band will preferentially hop into states at the low-energy side of the  $n=1$  band. We have thus an indirect generation of excitons in this low-energy region of the  $n=1$  band where the excitons are again blocked within their radiative lifetime.

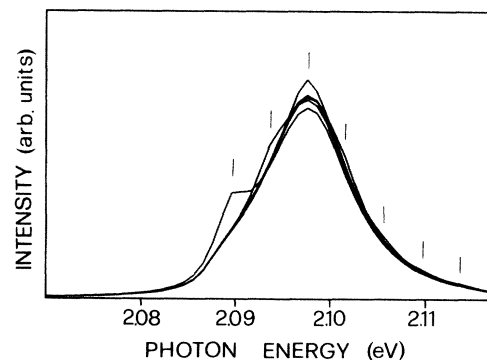


FIG. 8. Calculated photoluminescence spectra at 300 K for different excitation energies. The corresponding excitation energies are indicated by the vertical lines.

The calculated PL spectra for room temperature are shown in Fig. 8. We see that at this temperature the PL spectra become nearly independent of the excitation energy, in perfect agreement with experiment. This behavior is easily explained in terms of our model: At high temperature the transition rates between the different states become very large, and the excitons thermalize rapidly and distribute over a wide range of states.

The linewidth of the calculated PL spectra as well as their position in energy differ with respect to the experimental results presented in Fig. 4: The calculated linewidth is much too small (15 meV instead of 33 meV). This is expected, since we did not consider any temperature dependence of the broadening parameter  $\Gamma$ , which would account for the decrease of the exciton lifetime due to exciton-phonon coupling. Similarly, the position of the calculated PL spectra must be corrected for the decrease of the gap due to the electron-phonon coupling, which is about 90 meV between 80 and 300 K.<sup>14</sup>

### VIII. CONCLUSIONS

We have shown that the experimentally found freezing in of excitations into the low-energy side of the exciton absorption band, which is found at low temperatures, can be understood as a consequence of the localization of the

$n = 1$  excitons due to the presence of stacking disorder. The relative red shift of the DFE PL and the increase of the PL linewidth, which are observed for excitation energies beyond the maximum of the DFE absorption line, are both related to the contributions from secondary excitons, which become important for excitation into this energy range.

Our model does also explain the dependence of the PL on the temperature: The independence of the PL spectra on the excitation energy, which is found at room temperature, is due to the fact that at this temperature the excitons can easily hop from one site to another and change their energy by interaction with the phonon bath. In other words, for large temperatures the thermalization processes are much faster than the direct recombination processes.

### ACKNOWLEDGMENTS

We express our thanks to H. Berger and F. Lévy for providing us the GaSe samples, and to M. Montagna for stimulating discussions. This work was supported in part by the Fonds National de la Recherche Scientifique of Switzerland and by the Consiglio Nazionale delle Ricerche of Italy, Contract No. 85. 00355.02.

<sup>1</sup>E. Cohen and M. D. Sturge, Phys. Rev. B **25**, 3828 (1982).

<sup>2</sup>J. Hegarty, L. Goldner, and M. D. Sturge, Phys. Rev. B **30**, 7346 (1984).

<sup>3</sup>V. Capozzi, S. Caneppele, and M. Montagna, J. Lumin. **31/32**, 463 (1984).

<sup>4</sup>B. Movaghar, M. Grünewald, B. Ries, H. Bässler, and D. Würtz Phys. Rev. B **33**, 5545 (1986).

<sup>5</sup>K. Maschke and Ph. Schmid, Phys. Rev. B **12**, 4312 (1975); K. Maschke and H. Overhof, *ibid.* **15**, 2058 (1977).

<sup>6</sup>J. J. Forney, K. Maschke, and E. Mooser, J. Phys. C **10**, 1887 (1977).

<sup>7</sup>K. Maschke, E. Merk, and W. Czaja, Helv. Phys. Acta **58**, 417 (1985); J. Non-Cryst. Solids **77/78**, 687 (1985).

<sup>8</sup>Le Chi Thanh and C. Depeursinge, Solid State Commun. **25**, 499 (1978); Y. Sasaki and Y. Nishina, Physica **105B**, 45 (1981); X. C. Zhang, M. Gal, and A. V. Nurmikko, Phys. Rev. B **30**, 6214 (1984).

<sup>9</sup>Ph. Schmid, J. P. Voitchovsky, and A. Mercier, Phys. Status Solidi A **21**, 443 (1974).

<sup>10</sup>V. Capozzi, G. Mariottio, M. Montagna, A. Cingolani, and A. Minafra, Phys. Status Solidi A **40**, 93 (1977).

<sup>11</sup>G. Gobbi, J. L. Staehli, M. Guzzi, and V. Capozzi, Helv. Phys. Acta **52**, 337 (1979).

<sup>12</sup>V. Capozzi, Phys. Rev. B **23**, 836 (1981); V. Capozzi, S. Caneppele, M. Montagna, and F. Lévy, Phys. Status Solidi B **129**, 247 (1985).

<sup>13</sup>We note that GaSe is an indirect semiconductor. The indirect gap is only 25 meV lower than the direct one. The binding energy is equal to 20 meV for the direct exciton and  $\sim 30$  meV for the indirect exciton [see Ref. 12 and Le Chi Thanh and C. Depeursinge, Solid State Commun. **21**, 317 (1977)].

<sup>14</sup>Ph. Schmid and J. P. Voitchovsky, Phys. Status Solidi B **65**, 249 (1974).